

Fabrication of 50 nm period gratings with multilevel interference lithography

Chih-Hao Chang,* Y. Zhao, R. K. Heilmann, and M. L. Schattenburg

Space Nanotechnology Laboratory, Massachusetts Institute of Technology, Cambridge, Massachusetts 02139, USA

*Corresponding author: chichang@mit.edu

Received April 24, 2008; revised June 4, 2008; accepted June 5, 2008;
posted June 16, 2008 (Doc. ID 95394); published July 10, 2008

We have developed a multilevel interference lithography process to fabricate 50 nm period gratings using light with a 351.1 nm wavelength. In this process multiple grating levels patterned by interference lithography are overlaid and spatial-phase aligned to a common reference grating using interferometry. Each grating level is patterned with offset phase shifts and etched into a single layer to achieve spatial-frequency multiplication. The effect of the multilayer periodic structure on interference lithography is examined to optimize the fabrication process. This process presents a general scheme for overlaying periodic structures and can be used to fabricate more complex periodic structures. © 2008 Optical Society of America

OCIS codes: 050.2770, 220.4241, 110.4235.

High-density grating structures have applications in many research areas, including x-ray and extreme ultraviolet spectroscopy [1–3], subwavelength optics [4], atom diffraction [5], and templates for self-assembly [6]. There are a number of important factors in describing periodic structures, including grating period, spatial-phase coherence, linewidth control, and patterned area size. Depending on the application, emphasis is placed on different factors.

Interference lithography is an attractive method for fabricating grating structures, as it offers several advantages including a large exposure area and high spatial-phase coherence. However, the spatial resolution is limited by the light source, and the smallest attainable period is $\lambda/2n$, where λ is the light source wavelength and n is the refractive index of the medium. Shorter wavelength lasers and immersion techniques have been used to fabricate gratings with sub-50 nm periods [7,8], but these methods require complex sources and have limited exposure area. Other nonoptical fabrication processes have been demonstrated to multiply the spatial frequency of patterned gratings by an even factor down to a 50 nm period [9,10], but the process is limited to one-dimensional patterns.

This Letter presents an alternative spatial-frequency multiplication process based on the concept of multiple exposures [11]. In this process several levels of grating patterns are aligned with high accuracy to produce a grating with a 50 nm period. Using this process the wavelength-limited resolution in interference lithography can be extended with high-precision metrology and well-controlled fabrication techniques.

Our fabrication process is illustrated in Fig. 1. Initially, a silicon nitride reference grating with a period of $p=200$ nm is patterned in the outer region of a substrate using interference lithography ($\lambda=351.1$ nm). This reference grating then serves as a fiducial pattern for subsequent lithography steps [12]. Photoresist and antireflection coating (ARC) are then spun onto the substrate, as shown in Fig. 1(a).

The first grating level, also with a period of $p=200$ nm, is aligned and exposed at a relative phase-offset to the reference grating, with linewidth w . The grating pattern is then transferred into the nitride layer, as depicted in Figs. 1(b) and 1(c). The process is then repeated, as shown in Figs. 1(d) and 1(e), with

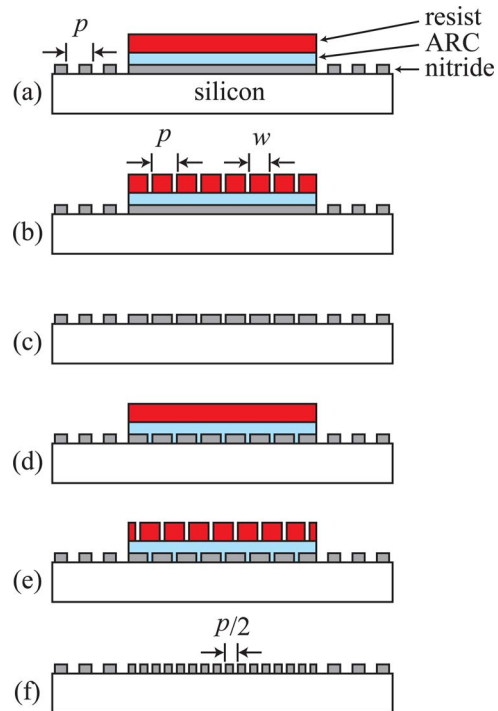


Fig. 1. (Color online) Fabrication process diagram for multilevel interference lithography. (a) A reference grating is patterned in the outer substrate region, while the center region is spincoated with ARC and photoresist. (b) After aligning to the reference grating, the first grating level with period $p=200$ nm is patterned. (c) The pattern is transferred into nitride. (d) After spincoating ARC and photoresist, (e) the second grating level is exposed at an additional π phase-offset. (f) The grating is pattern transferred, resulting in a nitride grating with a period of $p/2=100$ nm.

the second grating level exposed at an additional π phase-offset. After pattern transfer, the nitride grating has a resulting period of $p/2=100$ nm. Depending on the duty-cycle w/p of each grating level, the process can be repeated to further reduce the period.

The main challenges of this multilevel process are phase overlay accuracy, linewidth control, and layer design of each grating level. To achieve accurate overlay alignment, the phase of the reference grating is mapped prior to lithography so that each grating level can be exposed at the desired phase shift. The phase of the reference grating is measured by two beams at the same incident angles as during lithography, satisfying the Littrow condition. Thus the zeroth-order reflection of one beam and the backdiffracted first order of the other beam copropagate and interfere, providing a phase signal. The reference grating is designed with 45 nm of silicon nitride so that the diffracted orders are balanced in intensity to optimize the phase signal. This alignment method is implemented using the MIT nanoruler [13], and overlay accuracy of -1 ± 2.8 nm has been achieved over $35\text{ mm}\times 25\text{ mm}$ areas [14].

As a prerequisite for high spatial-frequency multiplication factors, a high duty-cycle grating pattern with nanometer repeatability is needed for each grating level. To control the grating linewidth, an oxygen plasma etch is used to reduce the grating line until the desired target is reached. After trimming the linewidth, an image-reversal process is used to transfer the thin-line pattern into a high duty-cycle pattern. Using this process a grating pattern with a ~ 0.88 duty cycle can be patterned with repeatability of a few nanometers. At such high duty cycles four phase-shifted grating levels can be overlaid for four-fold spatial-frequency multiplication.

Another key issue of the multilevel interference lithography process is the optical effect of the layered periodic structure. In traditional interference lithography an ARC layer is typically used to decrease beam reflection at the photoresist-ARC interface to reduce standing waves during exposure. For homogeneous layers an optimal ARC thickness can be readily simulated using the transfer matrix method. In our multilevel process, however, the underlying grating allows additional propagation modes and may result in additional standing waves. These effects are important in designing an exposure photoresist stack for each exposure step.

We simulated the optical fields within the multilevel periodic structure using rigorous coupled-wave analysis (RCWA) [15–17]. In the multilevel process the exposure condition for each grating level is different, so four separate layer geometries are examined. The stack in all four cases consists of 220 nm of photoresist (Sumitomo PFI-88A2, $n=1.72-0.04j$), thickness t of ARC (Brewer Science i-CON-16, $n=1.646-0.398j$), and 45 nm of silicon nitride ($n=2.47-0.195j$) on top of silicon ($n=5.47-2.99j$). Depending on the exposure step the nitride layer is either a homogenous film or a periodic structure planarized by ARC. For an exposure beam ($\lambda=351.1$ nm) at an incident angle of 61.37° , the re-

lected efficiencies relative to the incident beam intensity at the photoresist-ARC interface are simulated as functions of ARC thickness t for the four cases, as shown in Fig. 2(a). Each simulating condition, from the first to the fourth grating level exposure, is illustrated in Fig. 2(b).

The first exposure is the case of interference lithography over homogenous layers, so there is only the reflected zeroth order. During the third exposure, the spatial frequency of the underlying grating has been doubled and the subwavelength structure yields only the reflected zeroth order. The underlying grating during the second exposure allows an additional propagating order, which has the same wave vector magnitude as the reflected order. The same is true during the fourth exposure, in which the underlying grating from the third exposure produces an additional propagating order. In the latter two cases the intensity of the grating-induced propagating order is relatively small compared to the reflected order and is weakened significantly by the ARC. To minimize the intensity of the dominant reflected order, ARC thicknesses from 120–130 nm have been chosen for the exposures.

A scanning electron micrograph of a spatial-frequency doubled grating using the multilevel interference lithography process is shown in Fig. 3. Using $\lambda=351.1$ nm, the sample was patterned twice with a 200 nm period grating. The resulting 100 nm period grating is etched into nitride. The phase overlay accuracy and linewidth variation between the two levels are typically both better than 5 nm over a $35\text{ mm}\times 20\text{ mm}$ area. The grating has the desired high duty-cycle profile required for the placement of subsequent levels. A third exposure can place another grating level between the two existing grating patterns, as shown in Fig. 4. This pattern demonstrates the versatility of the multilevel interference lithography process, in which 200 nm period grating patterns with feature sizes down to ~ 25 nm can be aligned and exposed at arbitrary phase shifts. The fourth exposure places the final grating level, resulting in a 50 nm period grating, as shown in Fig. 5.

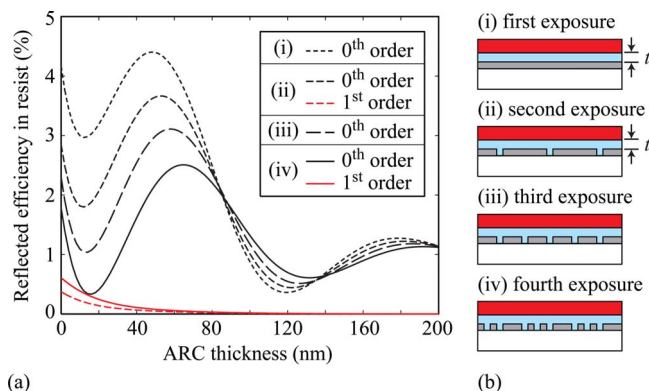


Fig. 2. (Color online) Simulated intensity efficiencies of the reflected orders at the photoresist-ARC interface with varying ARC thickness for the four exposure conditions. (b) The corresponding exposure conditions, each with 220 nm of photoresist, thickness t of ARC, and 45 nm of homogenous-periodic silicon nitride on top of silicon.

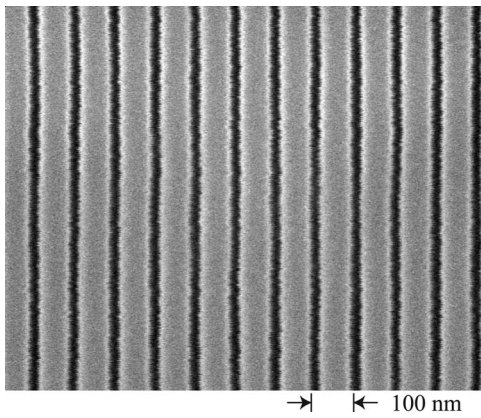


Fig. 3. 100 nm period grating fabricated by overlaying two 200 nm period grating levels.

Typically, for each level of lithography overlay accuracy and linewidth control to a few nanometers can be achieved over large areas. However, instability of process conditions and particle contamination limit

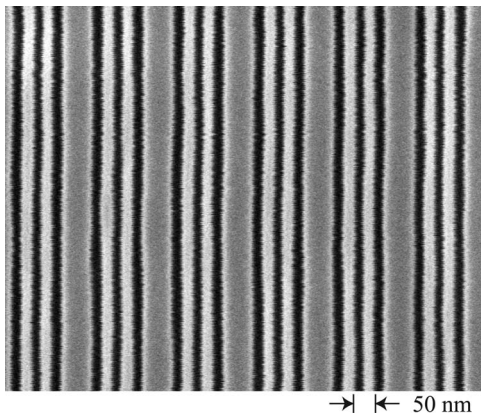


Fig. 4. Grating pattern fabricated by overlaying three 200 nm period grating levels.

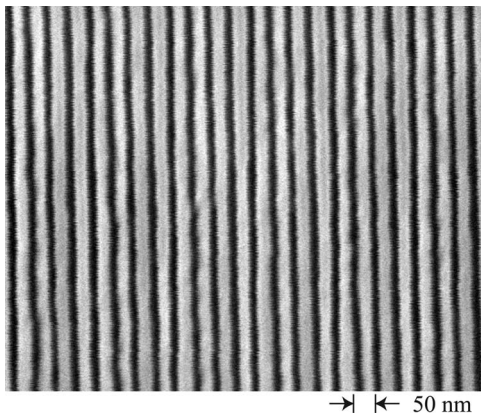


Fig. 5. 50 nm period grating fabricated by overlaying four 200 nm period grating levels.

yield in the university laboratory environment. In principle, by having tighter process control this multilevel process can be scaled to pattern 300 mm substrates. A closed-loop metrology scheme with real-time phase measurement would also increase the robustness of this process and is being explored.

In this Letter, a multilevel interference lithography fabrication process overlaying multiple grating levels has been presented. Using this process, four 200 nm grating levels have been overlaid to fabricate a grating with 50 nm period. More importantly, spatial-frequency multiplication is only one of many applications of this process. The ability to pattern multiple grating levels with ~ 25 nm feature sizes at arbitrary phase shifts is the main advantage of this process. By using two-dimensional reference patterns, complex three-dimensional nanostructures can be fabricated.

References

1. M. P. Kowalski, R. K. Heilmann, M. L. Schattenburg, C.-H. Chang, F. B. Berendse, and W. R. Hunter, *Appl. Opt.* **45**, 1676 (2006).
2. J. F. Seely, L. I. Goray, B. Kjornrattanawanich, J. M. Laming, G. E. Holland, K. A. Flanagan, R. K. Heilmann, C.-H. Chang, M. L. Schattenburg, and A. P. Rasmussen, *Appl. Opt.* **45**, 1680 (2006).
3. D. Hambach, G. Schneider, and E. M. Gullikson, *Opt. Lett.* **26**, 1200 (2001).
4. Y. Kanamori, M. Sasaki, and K. Hane, *Opt. Lett.* **24**, 1422 (1999).
5. D. W. Keith, M. L. Schattenburg, H. I. Smith, and D. E. Pritchard, *Phys. Rev. Lett.* **61**, 1580 (1988).
6. J. Y. Cheng, C. A. Ross, E. L. Thomas, H. I. Smith, and G. J. Vancso, *Appl. Phys. Lett.* **81**, 3657 (2002).
7. T. M. Bloomstein, M. F. Marchant, S. Deneault, D. E. Hardy, and M. Rothschild, *Opt. Express* **14**, 6434 (2006).
8. H. H. Solak, C. David, J. Gobrecht, V. Golovkina, F. Cerrina, S. O. Kim, and P. F. Nealey, *Microelectron. Eng.* **67-68**, 56 (2003).
9. Z. Yu, W. Wu, L. Chen, and S. Y. Chou, *J. Vac. Sci. Technol. B* **19**, 2816 (2001).
10. B. Cui, Z. Yu, H. Ge, and S. Y. Chou, *Appl. Phys. Lett.* **90**, 043118 (2007).
11. S. R. J. Brueck, *Proc. IEEE* **93**, 1704 (2005).
12. M. L. Schattenburg, C. Chen, P. N. Everett, J. Ferrera, P. Konkola, and H. I. Smith, *J. Vac. Sci. Technol. B* **17**, 2692 (1999).
13. R. K. Heilmann, C. G. Chen, P. T. Konkola, and M. L. Schattenburg, *Nanotechnology* **15**, S504 (2004).
14. Y. Zhao, C.-H. Chang, R. K. Heilmann, and M. L. Schattenburg, *J. Vac. Sci. Technol. B* **25**, 2439 (2007).
15. M. G. Moharam, E. B. Grann, D. A. Pommet, and T. K. Gaylord, *J. Opt. Soc. Am. A* **12**, 1068 (1995).
16. M. G. Moharam, D. A. Pommet, E. B. Grann, and T. K. Gaylord, *J. Opt. Soc. Am. A* **12**, 1077 (1995).
17. W. Lee and F. L. Degertekin, *J. Lightwave Technol.* **22**, 2359 (2004).